

# Magnetic and structural properties of nanocrystalline $\text{PrCo}_3$ .

K Younsi<sup>1</sup>, V Russier<sup>1</sup>, L Bessais<sup>1</sup>, J-C Crivello<sup>1</sup>

<sup>1</sup> ICMPE, UMR 7182 CNRS-Université Paris Est,

2-8 Rue Henri Dunant F-94320 Thiais, France.

russier@icmpe.cnrs.fr

## Abstract

The structure and magnetic properties of nanocrystalline  $\text{PrCo}_3$  obtained from high energy milling technique are investigated by X-ray diffraction, Curie temperature determination and magnetic properties measurements are reported. The as-milled samples have been annealed in a temperature range of 1023 K to 1273 K for 30 mn to optimize the extrinsic properties. The Curie temperature is 349 K and coercive fields of 55 kOe at 10 K and 12 kOe at 293 K are obtained on the samples annealed at 1023 K. A simulation of the magnetic properties in the framework of micromagnetism has been performed in order to investigate the influence of the nanoscale structure. A composite model with hard crystallites embedded in an amorphous matrix, corresponding to the as-milled material, leads to satisfying agreement with the experimental magnetization curve. [ K. Younsi, V. Russier and L. Bessais, J. Appl. Phys. **107**, 083916 (2010)]. The microscopic scale will also be considered from DFT based calculations of the electronic structure of  $R\text{Co}_x$  compounds, where  $R = (\text{Y}, \text{Pr})$  and  $x = 2, 3$  and 5.

## 1 Introduction

The permanent magnetic materials with high performance require appropriate intrinsic hard magnetic properties *i.e* a high uniaxial magnetocrystalline anisotropy field, a high Curie temperature and a high saturation magnetization. Among nanocrystalline magnets based on rare earth and transition metal compounds the  $R\text{Co}_3$  compounds ( $R$  as a rare earth) have been the subject of many studies during the last decades. These ones crystallize in rhombohedral  $\text{PuNi}_3$ -type (space group:  $R\bar{3}m$ ). The unit cell contains two non-equivalent crystallographic sites for  $R$  ions,  $3a$  and  $6c$ , and three sites for Co:  $3b$ ,  $6c$  and  $18h$ .  $R\text{Co}_3$  alloys present excellent magnets properties such as large magnetocrystalline anisotropy and important saturation magnetization. These properties are resulting from to combination of the  $3d$  itinerant magnetism of the Co sublattice and  $4f$  localized magnetism of the sublattice.

In this study, we report the elaboration of nanocrystalline  $\text{PrCo}_3$  by high-energy milling, and their structural and magnetic properties in amorphous state and after recrystallization. Hard magnetic properties of the as milled  $\text{PrCo}_3$  have been improved by a controlled nanocrystallization, which optimize the grain size in order to obtain a high coercivity.

In addition to the experiments, results from simulation and microscopic calculations are presented. We have proposed a simple model for the system after annealing based on a lattice of crystallites embedded in an amorphous matrix. The simplest realization of such a model is considered here, in order to bring out at the qualitative level the microstructure effect on the magnetization curve. This model is treated in the framework of micromagnetism, *i.e.* through a continuous medium type of approach, and the calculations are performed by using the MAGPAR [1] code based on the finite elements method. We also present the results of *ab initio* band structure calculations and magnetic properties based on the spin polarized local approximation of the density functional theory (DFT) of  $R\text{Co}_x$ , where  $R=(\text{Y},\text{Pr})$  and  $x=2,3$  and 5 intermetallic compounds. We will focus on a quantitative analyse of the localized  $4f$  states and itinerant  $3d$  magnetism.

## 2 Experimental studies

A polycrystalline  $\text{PrCo}_3$  was prepared by melting high-purity starting elements ( $> 99.9\%$ ) in an induction furnace under an atmosphere of high purity Ar. The ingot was remelted five times to ensure homogeneity. These ingots were used as pre-alloys to manufacture samples by high-energy milling. Technique and conditions of milling has been described in [2]. After milling, the powder mixtures was wrapped in tantalum foil and sealed in silica tubes under a vacuum of  $10^{-6}$  Torr, then annealed for 30 min at temperature between 1023 K and 1323 K followed by quenching in water. X-ray diffraction (XRD) patterns of as-cast, as-milled and annealed powders were carried out with Cu-K $\alpha$  radiation source on a Bruker diffractometer. The unit-cell parameters were measured with Si as the standard ( $a= 5.4308 \text{ \AA}$ ) leading to a unit-cell parameter accuracy of  $\pm 1 \times 10^{-3} \text{ \AA}$ . The data treatment was made by Rietveld refinement with FULLPROF computer code in the assumption of ThompsonCox-Hastings line profile alloying multiple-phase refinement. This refinement gives the weight percentage of each of the coexisting phases, the line broadening leads to the autocohrent domain size owing to Scherrer formula. The magnetic ordering temperatures  $T_C$  were obtained on a differential sample magnetometer MANICS in a field of 1 kOe on powder, in vacuum-sealed silica tube. Curie temperature was determinate by extra-polating the linear part of the MT curve and extending the baseline: intersection point corresponds to the value of  $T_C$ . The  $M - H$  curves (Magnetic hysteresis measurement) were plotted at  $T= 10$  and 293 K with a Physical Properties Measurement System (PPMS) Quantum Design equipment and a maximum applied field of 90 kOe on sample in epoxy resin.

### 2.1 Structure analysis

Before milling, the ingot is analyzed by X-ray diffraction (XRD). The Fig. 1 presents the analysis result of XRD pattern of  $\text{PrCo}_3$  ingot using the Rietveld analysis. The  $\text{PrCo}_3$  ingot is nearly single phase with the rhombohedral  $\text{PuNi}_3$ -type structure (space group:  $R\bar{3}m$ ) and is an appropriate precursor for

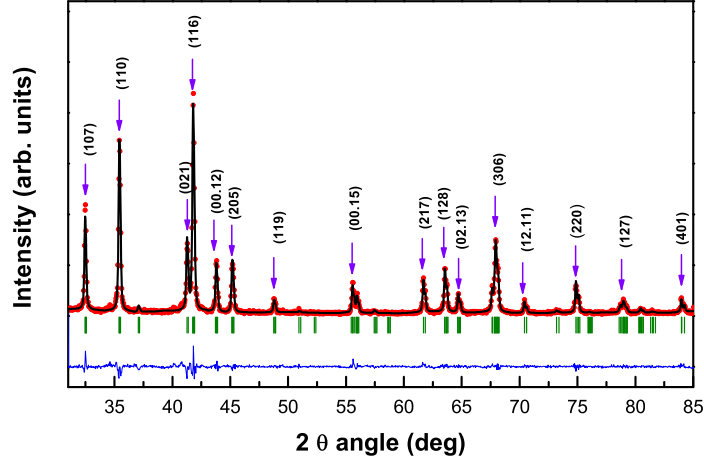


Figure 1: Rietveld analysis for  $\text{PrCo}_3$  ingot.

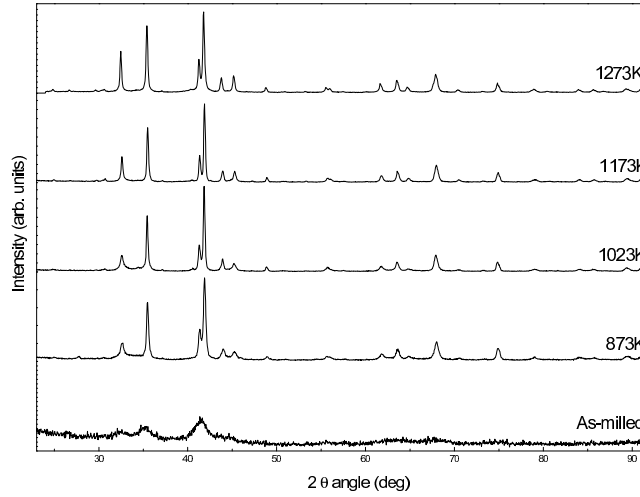


Figure 2: XRD pattern of the  $\text{PrCo}_3$  as-milled and annealed samples at 773 and 1273 K during 30 min.

using as pre-alloys to manufacture samples by high-energy milling.

In order to check the crystalline structure of  $\text{PrCo}_3$  powders, the XRD measurement of samples annealed at distinct temperature have been performed. The XRD patterns of both as-quenched and annealed  $\text{PrCo}_3$  powder are shown in Fig.2. It can be seen that as-quenched powder is essentially quasicrystalline. Such quasicrystalline matrix suggests the presence of various types of small crystallites. The diffraction peaks become more pronounced with increasing annealing temperature. The annealed samples at 773 and 1273 K for 30 min reveal the presence of  $\text{PrCo}_3$  phases crystallized.

However, when the annealed is at temperature between 773 and 1023 K, we observe in the low angles a large line around  $32^\circ$ . The large peak widths points to a small grain size. When the powders are annealed at temperature higher than 1023 K, the XRD patterns show the presence of  $\text{PrCo}_3$  phases crystallized. We have observed a small amount (around 0.5 wt%) of  $\text{Pr}_2\text{O}_3$  in all samples annealed after milling. The mean diffraction crystallite size of the powder after annealing at 1023 and 1273 K for 30 min obtained by fitting the XRD diagram with Rietveld method, ranges between 31 and 45 nm respectively, this implies that synthesized materials are noncrystalline.

The Curie temperature is determined by the exchange-coupling interaction between the nearest-neighbor Co-Co atoms, which is the origin of ferromagnetism. This interaction depends markedly on the interatomic distance. The Curie temperature of  $\text{PrCo}_3$  compound is 349 K, [2] this result is in agreement with the data given by Lemaire [3].

The low Curie temperature in  $\text{PrCo}_3$  compounds is due to the short Co-Co interatomic distances at the sites  $6c - 18h$  and at  $18h - 18h$  [2], where the Co atoms couple antiparallel. In this structure, the  $6c - 18h$  and at  $18h - 18h$  interactions are strongly negative.

Isothermal magnetization curves  $M - H$  obtained at 293 K is represented in Fig. 3 for  $\text{PrCo}_3$ . This figure shows that at 293 K the saturation is not reached, which gives evidence for a magnetocrystalline anisotropy among the highest known in those kinds of systems. The pattern obtained on sample oriented under an external magnetic field, applied perpendicularly to the plane of the sample, shows only  $(00l)$  Bragg peaks, which amount to suggest that the anisotropy strengthens the peaks of diffraction of type  $(00l)$  and at room temperature the easy magnetization direction is parallel to the  $c$ -axis. A similar result is obtained for  $\text{YCo}_{3-x}\text{Fe}_x$  by [4] obtained by oriented powder under extern field.

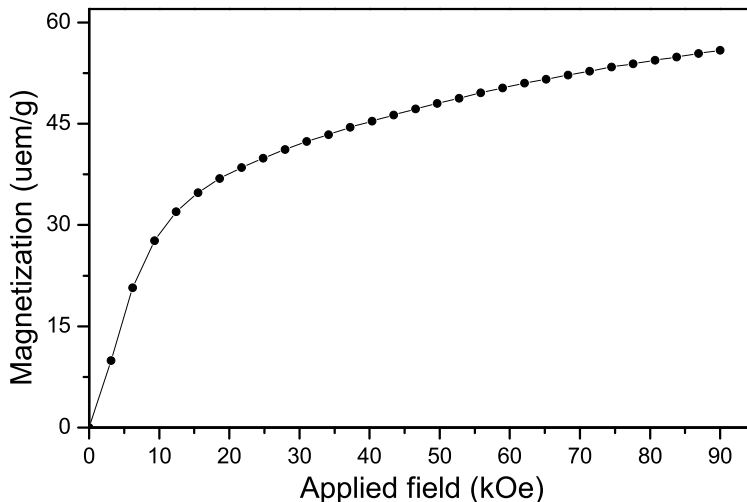


Figure 3: Magnetization curves of  $\text{PrCo}_3$  obtained after high-energy milling and annealed at  $750^\circ\text{C}$  for 30 min, measured at 293 K.

## 2.2 Extrinsic magnetic properties

The best magnetic properties were reached after a treatment at 1023 K for 30 min. Fig. 4 show as an example the hysteresis loops measured at 10 and 293 K. This sample exhibits the highest coercivities we have obtained, for  $T = 10$  K,  $H_c = 55$  kOe,  $M_R = 56$  emu/g and  $M_R/M_{\text{max}} = 0.75$ . For  $T = 293$  K,  $H_c = 12$  kOe and  $M_R = 44$  emu/g and  $M_R/M_{\text{max}} = 0.60$  inherent to nanocrystalline state. The highest coercivity of 55 kOe at 10 K confirms the large magnetocrystalline anisotropy.

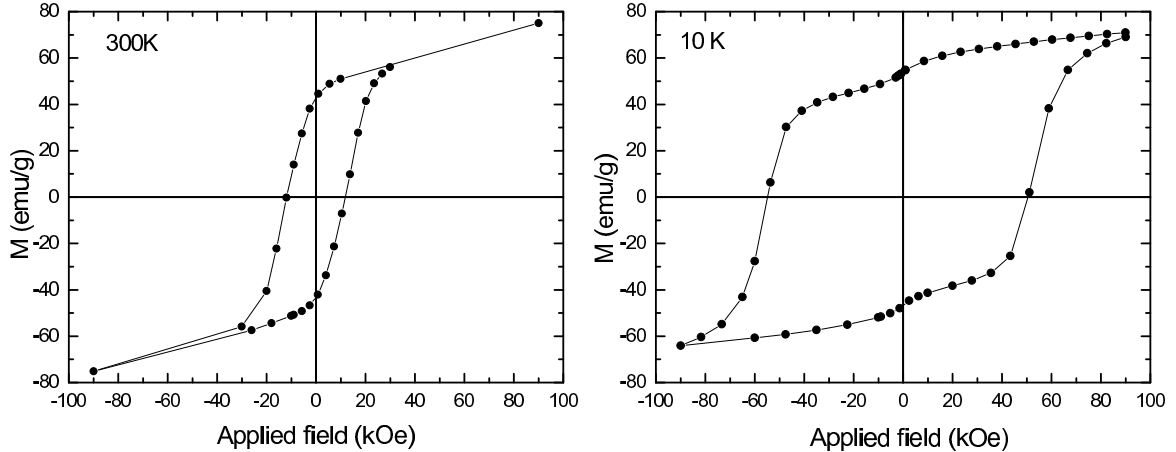


Figure 4: Hysteresis loop of  $\text{PrCo}_3$  milling before and after annealing at 1023 K for 30 min, measured at 293 and 10 K.

### 3 Computational studies

#### 3.1 Micromagnetism simulation

In order to get a picture of the link between the structure at the nanometer scale and the extrinsic magnetic properties we have performed a micromagnetic simulation on a model for the system. The picture we have in mind is that the crystallization takes place locally on dispersed seeds in the amorphous matrix representing the as-milled sample. Hence we consider an assembly of crystallites presenting a uniaxial anisotropy comparable to what is expected in hard magnetic R-TM compounds. The saturation magnetization,  $J_s$  of the crystallites is that of the bulk  $\text{PrCo}_3$ , namely  $J_s = 0.723 \text{ T}$ . We consider the simplest realization of the model, by using identical crystallites, located on the nodes of a simple cubic lattice. The crystallites are either spherical or cubic; however, the later case is likely to be closer to the experimental sample. We have chosen somewhat arbitrarily a volumic fraction occupied by the crystallites of  $\phi = 0.73$  (in the case of cubic crystallites) and the crystallite size corresponds to what has been estimated experimentally, namely, a cubic edge  $a = 35 \text{ nm}$ . The amorphous character of the matrix is translated by a zero valued anisotropy constant, while its saturation magnetization ( $J_s^{(mat)}$ ) is a free parameter of the model. The value we get for  $J_s^{(mat)}$ , namely c.a.  $J_s/5$  seems reasonable in our picture of an amorphous matrix. The important point is that we clearly get the signature of a two uncoupled phases behavior for  $M(H)$ ; the amplitude of the kink at zero field being determined by  $\phi$  and  $J_s^{(mat)}$ .

#### 3.2 DFT calculations

##### 3.2.1 Methodology

Band structure spin polarized calculations were carried out by using the DFT scheme implemented in the projector-augmented wave (PAW) method, performed with the VASP package [5, 6]. In the

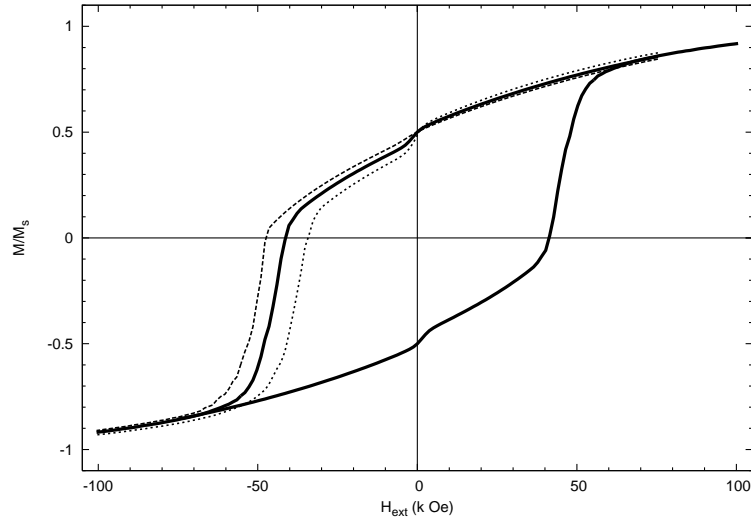


Figure 5: Calculated de-magnetization curve in terms of the external field for the systems of cubic inclusions with  $\varphi = 0.73$ . Randomly distributed axes and matrix saturation magnetization  $J_s = 0.05$  T, dashed line;  $J_s = 0.125$  T, solid line and  $J_s = 0.25$  T, dotted line.

present study, the generalized gradient approximation (GGA) is used for the exchange and correlation energy functionals with the Perdew-Burke-Ernzerhof (PBE) [7] functional. A plane wave basis set with a cutoff energy of 600 eV was used in all calculations converged within 0.1 eV in total energy. Brillouin zone sampling using a mesh of 0.5k points for each primitive cell of  $R\text{Co}_x$  compounds, described respectively in  $Fd\bar{3}m$  space group for  $x=2$ ,  $R\bar{3}m$  for  $x=3$  and  $P6_3/mmm$  for  $x=5$  compounds. Structural optimization were carried out under the condition that residual forces should be smaller than  $0.1 \text{ eV} \cdot \text{\AA}^{-1}$ .

### 3.2.2 Electronic structures

Figure 6 shows the density of states (DOS) for the  $\text{YCo}_x$  and  $\text{PrCo}_x$  ( $x=2, 3$  and  $5$ ) in the two directions of spin. For both series, the majority occupied states are dominated by the  $3d$  states of Co, with a small electronic charge transfert of  $R$  to Co, which is more important from  $R=\text{Y}$  to Co than from Pr to Co (calculated by Bader's theory). The increase of  $x$  leads to a distinct shift of the Co- $3d$  states in spin majority and minority DOS as expected in the rigid-band Stoner theory. Whereas  $R\text{Co}_2$  shows the paramagnetic state as the most stable in energy, the ferromagnetic behavior is confirmed for  $x=3$  and  $x=5$  compounds, with an increase of the angular magnetic moment from 1.45 to 7.34 and 3.59 to  $4.70 \mu_B \text{ f.u.}^{-1}$  for  $R=\text{Y}$  and Pr respectively. The magnetic anisotropy has been confirmed for  $R\text{Co}_3$  compounds, since non-collinear spin calculation along the  $z$  axis has been found  $\sim 0.2 \text{ eV f.u.}^{-1}$  more stable than calculation along  $x$  axis direction. Since the DOS at Fermi level is high enough for  $x=3$  and  $5$ , the itinerant magnetism properties of these compounds can be explained by intra-atomic  $3d - 3d$  exchange. In contrast to  $\text{YCo}_x$ ,  $\text{PrCo}_x$  compounds present tiny and high density structures above the Fermi level, corresponding to localized empty  $4f$  states of Pr. It is clear that the Co- $3d$

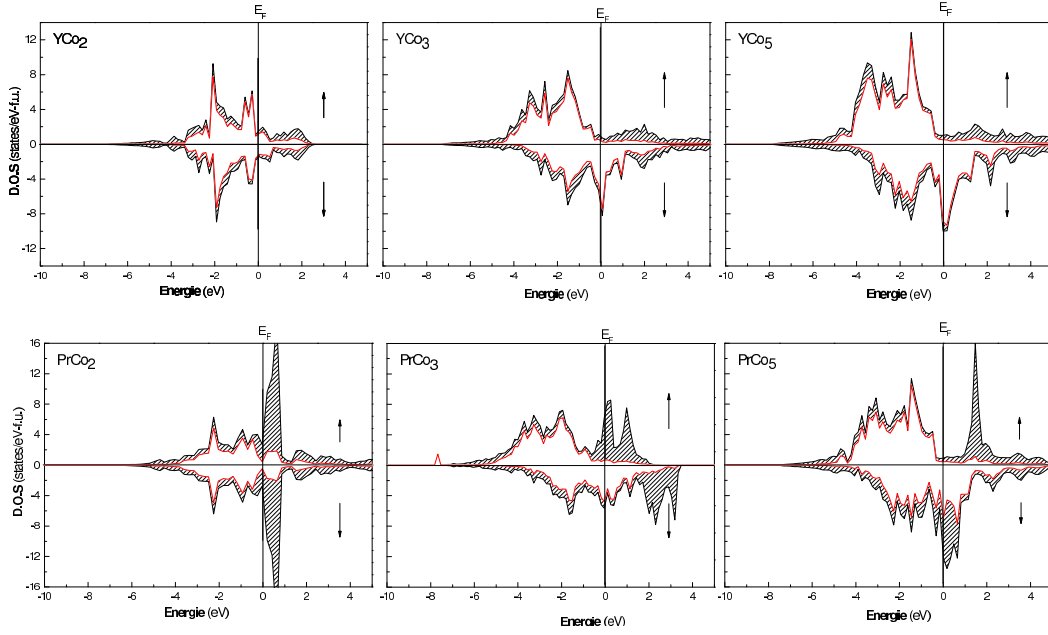


Figure 6: Total density of states (shaded region) of  $R\text{Co}_x$  ( $R=\text{Y}, \text{Pr}$  ;  $x=2, 3$  and  $5$ ). The white area is corresponding to the only  $3d$ -states of  $\text{Co}$ . The origin of the energy scale is located at the Fermi energy  $E_F$ .

states are modified compared to  $\text{YCo}_x$ , due to the hybridization with the  $\text{Pr-}4f$  states. As expected in  $3d - 5d$  hybridization compounds, the energy between the bonding and anti-bonding sub-bands becomes different for the two-direction of spins [8]. The consequence is a larger occupation of minority  $5d$  states as compared to majority  $5d$  of the rare earth, that means a ferrimagnetic coupling between  $3d$  and  $5d$  states occurs and increases with the increasing of  $x$  composition.

## 4 Conclusion and outlook

The  $\text{PrCo}_3$  intermetallic compound crystallizes in rhombohedral  $\text{PuNi}_3$ -type structure and presents a very high uniaxial magnetocrystalline anisotropy. The coercivity of this compound, prepared by high energy milling followed by annealing (1023 K, 30 mn), takes a very high value, up to 55 kOe at 10 K. A micromagnetic simulation and atomic scale *ab-initio* calculations have been performed to understand on the one hand the way in which the electronic structure and especially the interplay between  $3d$  and  $4f$  electronic states, leads to the observed anisotropy and magnetic moment, and on the other hand the relation between the nanoscale structure and the extrinsic magnetic properties. DFT calculations will be improved with spin-orbit coupling considerations, and with Hubbard corrections in order to better describe cohesive properties of materials with strong electronic correlations.

## Acknowledgement

The numerical part of this work was performed using HPC resources from GENSI- CINES (Grant 2010-096180).

## References

- [1] W. Scholz, T. Schrefl, D. Suess, R. Dittrich, H. Forster, and V. Tsiantos. *Comput. Mater. Sci.*, 28:366, 2003.
- [2] K. Younsi, V. Russier, and L. Bessais. *J. Appl. Phys.*, 107:083916, 2010.
- [3] R. Lemaire. *Cobalt*, 33:201, 1966.
- [4] M. I. Bartashevich, Tsuneaki. Goto, and Katsuhiko. Koui. *Physica B*, 292(1-2):9, October 2000.
- [5] G. Kresse and J. Furthmüller. Efficient iterative schemes for ab initio total-energy calculations using a plane-wave basis set. *Phys. Rev. B*, 54(16):11169–11186, Oct 1996.
- [6] G. Kresse and D. Joubert. From ultrasoft pseudopotentials to the projector augmented-wave method. *Phys. Rev. B*, 59(3):1758, 1999.
- [7] John P. Perdew, Kieron Burke, and Matthias Ernzerhof. Generalized gradient approximation made simple [phys. rev. lett. 77, 3865 (1996)]. *Phys. Rev. Lett.*, 78(7):1396, Feb 1997.
- [8] Manuel Richter. Band structure theory of magnetism in 3d-4f compounds. *J. Phys. D: Appl. Phys.*, 31(9):1017, 1998.